

FAST PARAMETRIC STRUCTURE MODELING FOR VARIETY OF AIRCRAFT CONFIGURATIONS

Yun-Long Yin^{1,2}, Ke-Shi Zhang^{1,2}, Hai-Long Qiao^{1,2}, Ai-Ling Che^{1,2} & Zhong-Hua Han^{1,2}

¹School of Aeronautics, Northwestern Polytechnical University, Xi'an, 710072, P.R.China ²National Key Laboratory of Aircraft Configuration Design, Xi'an, 710072, P.R.China

Abstract

Common parametric modeling is essential for aircraft design optimization process. It not only affects quality of the mesh, but also decides how efficiently the model can be updated. Based on most of the CAD models generated by the current methods, the preprocess is inevitable before mesh generation and design zones division is not so easy. In this work, we propose a new way of parametric structure modeling for variety of aircraft configurations, which is noted as surface discretization modeling method. The CAD model is a combination of the discretized pieces corresponding to the design zones, then the preprocess is not necessary and quality of the mesh can be easily improved. The proposed method is firstly validated by modeling a tailless fighter and compared with the refined model by hand, which obtains the satisfactory accuracy. Then the efficiency and practicality of this method is further demonstrated by the applications of the supersonic transport (SST), the tailless fighter and the flying-wing bomber.

Keywords: parametric modeling; surface discretization modeling; structural analysis

1. Introduction

Parametric modeling method is one of the critical technologies in the optimization of the aircraft design. Both the geometric model and the aircraft's internal structure must be updated when the design parameters are changed throughout the optimization process. That's why an automatic parametric modeling process need to be established.

Aerodynamic shape modeling and structural modeling are typically combined. Structural models are set up by building space relationships with the surfaces of geometric models generated by outer mold line (OML). The German Aerospace Center (DLR) developed a geometric modeler TiGL [1], which offers the functionality to export Common Parametric Aircraft Configuration Scheme (CPACS) geometries to standard CAD formats [2]. Based on it, the design environment for thin-walled lightweight structures (DELiS) [3] and ModGen [4] with the focus on structure mechanics and aeroelastics respectively are developed, and they have been widely applied in the research of commercial aircrafts[5], forward swept wing aircrafts [6], fighter aircrafts [7], etc. Klimmek et al. [8] further presented the aeroelastic structural design process cpacs-MONA, which is also part of highfidelity based MDO processes. OpenVSP [9] is a strong parametric geometry and analysis tool for conceptual aircraft design developed by NASA, which has been widely applied by various aircraft [10]-[13]. Martins et al. [14][15] developed an aircraft design tool, GeoMACH, for high-fidelity multidisciplinary analysis and optimization (MDAO), which generates inner structure by mapping the nodes of structural layout for components to physical space. Joe et al. [16] proposed a rapid parametric structure modeling method based on ESP [17], in which a parametric waffle structure is intersected with the OML to construct the structural model. However, it takes 10-15 minutes to obtain a new ESP model. Corrado et al. [18] established a structural parametric modeling platform Descartes and a composite thin-walled FEA Finite Element Analysis) platform Lagrange, which are more suitable for MDO of composite material wings for the next generation of Airbus aircraft. Van der Laan et al [19] developed a multimodel generator based on the ICAD software, that can transform a geometric model into a structural model by segmenting the movable model into easily meshable surfaces and storing information about material properties and loads. Xiongqing Yu et al. presented

a method to integrate CAD software with MDO, achieving the integration of aerodynamic/structure [20][21], aerodynamic/stealth design [22].

Coupling aerodynamic modeling with structural modeling can significantly improve the precision of the structural models. However, this will result in the problem of non-collinear adjacent areas and the inability to generate refined meshes on complex surfaces. Therefore, we separate the process of modeling aerodynamics from modeling structures and save the important points where these two models intersect. Instead of using geometric design parameters to create aerodynamic models, we now use them to establish mathematical connections with structural models. This approach can help reduce the time and effort required for modeling and generating meshes, but it will lead to a loss of precision. The present paper illustrates that a fast structure modeling method (Figure 1) facilitates the generation of low-fidelity model in a multidisciplinary design process.

The remainder of this paper is organized as follows: Section 2 focuses on the principle of surface discretization. The tailless fighter instance serves as a detailed demonstration of the parametric modeling procedure in Sections 3 and 4, where the accuracy of the model is validated. Section 5 provides the applications of SST, tailless fighter and flying-wing bomber, and Section 6 concludes the paper.

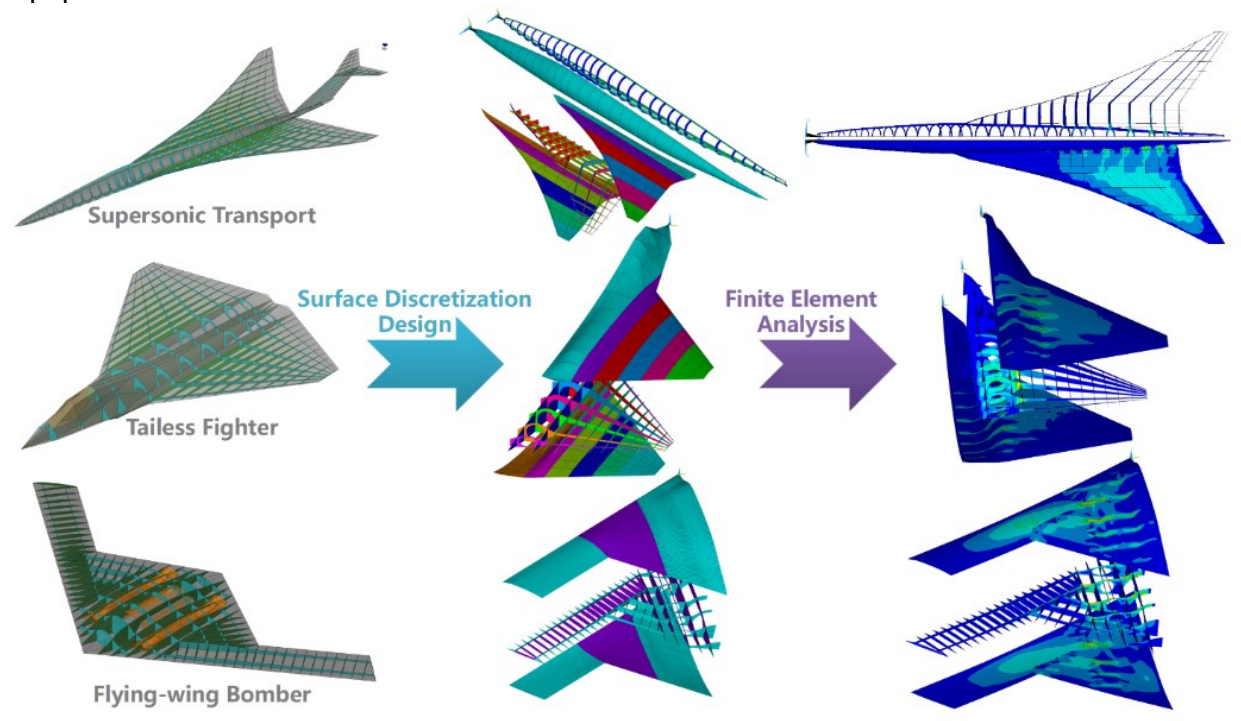


Figure 1 – Structure modeling process for complete aircraft configurations

2. Surface Discretization Modeling

The surface discretization modeling involves establishing the geometric model in a discretized manner at the beginning of the parametric modeling process, rather than discretizing it after the FEA is initiated, as depicted in Figure 2. In order to get high-quality mesh in the subsequent FEA, certain simplifications are made in the geometric modeling. Firstly, the large irregular surfaces are discretized into multiple relatively regular quadrilateral and triangular patches, such as wing ribs and fuselage bulkheads. Secondly, particular extensively curved surfaces, such as those located at the leading edge of the wing, are simplified by segmenting their outer model lines into multiple straight lines so that the curved surfaces become collections of small flat surfaces. In this way, the finite element mesh can fill the entire region without any gaps. In addition, it avoids fine meshing that is inevitable for the original highly-curved surface, hence enabling rapid meshing. By the way, when generating the geometric model, it is essential to ensure that adjacent surfaces have a common edge. This allows the associated finite element meshes to share nodes, maintaining uninterrupted force transmission channels on the structure.

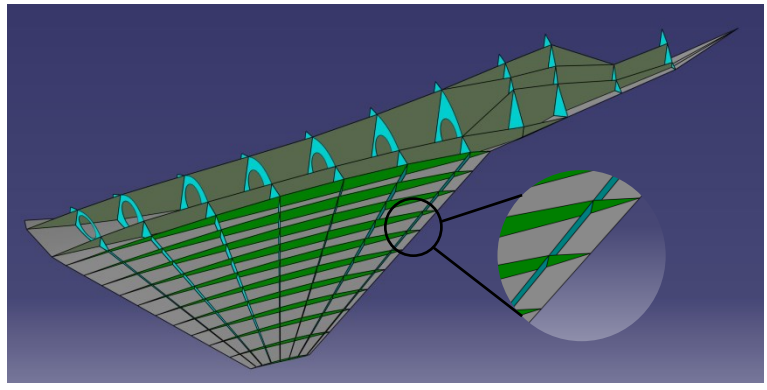


Figure 2 – Surface discretization modeling

Surface discretization modeling not only speeds up parametric modeling but also facilitates the grouping of design zones. Each individual surface can be taken as a single design unit to optimize thousands of variables, or be grouped into larger pieces to form design units when only a small amount of design variables is acceptable, as shown in Figure 3.

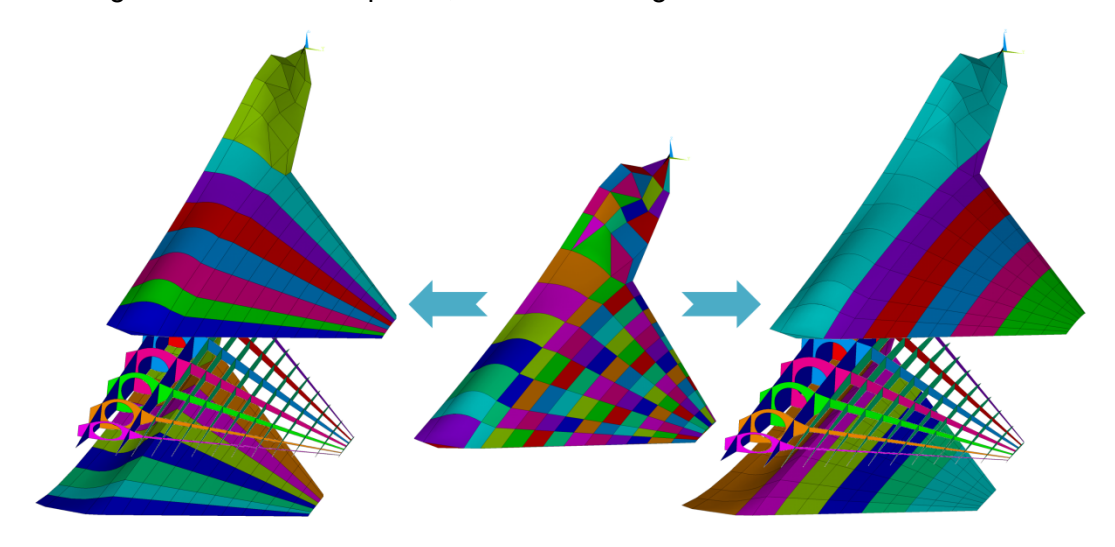


Figure 3 – Classification and merging of discretization surfaces

3. Parametric modeling process

The design and implementation of the parametric modeling process is based on macro scripts written in VB language. In order to adaptively generate and update the CAD models of aircraft configurations that may differ a lot from each other, the templates of different concepts are previously prepared. As shown in Figure 4, the template includes the geometric information of all the key points.

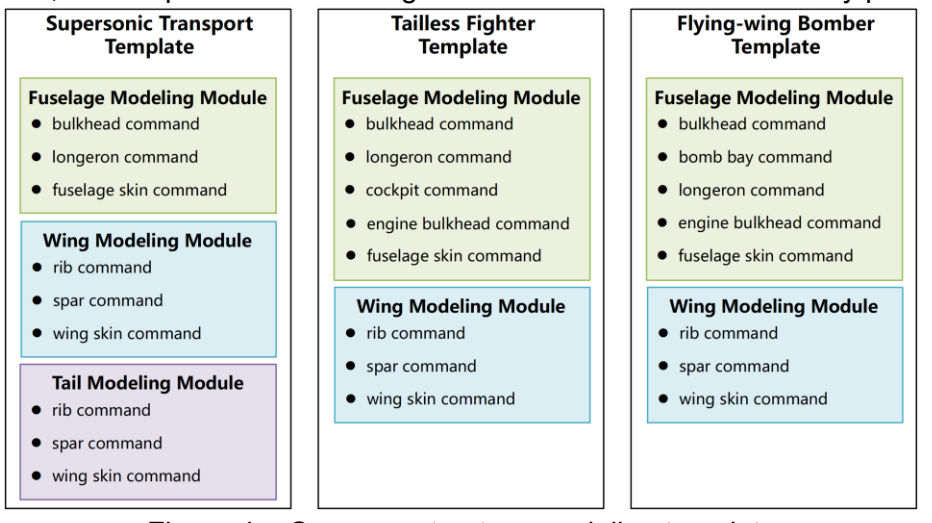


Figure 4 – Common structure modeling template

As shown in Figure 5, for any template, its modeling framework can be broadly divided into three parts: parameters input, model generation, and IGES output. In the first part, the plane parameters are used to control the configurations, while section parameters are for the specific shape. Then, model is generated from points to lines to surfaces. Finally, the generated surface model is exported to IGES format in order to proceed with the subsequent FEA stage.

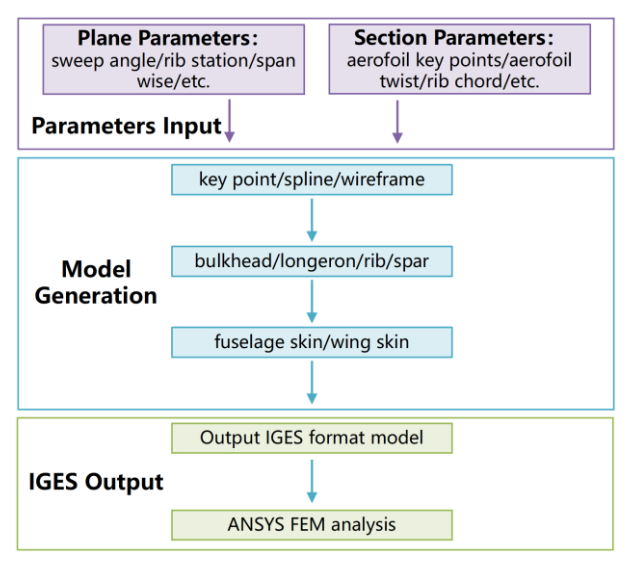


Figure 5 – Parametric modeling method framework

Table 1 shows the pseudocode of parametric modeling process and Figure 6 (a)-(h) demonstrates some key steps in generation of a tailless fighter model. Below is a detailed explanation of this process.

- 1) The plane parameters including configuration information and section parameters including profile information are read in through macro scripts. Subsequently, the program automatically creates key points by utilizing the corresponding geometric relationships, as illustrated in Figure 6(a). The key points of fuselage are generated at the bulkhead locations and are used to connect the fuselage contour lines in subsequent steps. The key points of a wing constitute a subset of the point set of an airfoil profile, while serving as points at the intersections of wing ribs and spars. The wing's plane and section information is reflected using the minimum number of points possible.
- 2) The overall outline and dimensions of the entire aircraft are basically determined after step 1. Then, the key points of the fuselage and wing are connected in a certain order using spline curves, thereby interpolating the outer contour lines of the fuselage and wing structure, as shown in Figure 6(b) and (c). In order to guarantee each outer contour line is independent and non-intersecting, it is necessary to divide a curve into several segments according to the number of key points on this curve. The fact that each segment has only two key points simplifies the modeling of surface discretization.
- 3) This step is to loft or fill surfaces based on these outer contour lines. It is worth noting that the discretized surfaces mean that a large irregular polygonal surface is discretized into a collection of surfaces composed only of quadrilaterals and triangles. This process is performed to automatically create meshes consisting of quadrilateral shell elements, which will be used for further FEA. Longitudinal structural components such as fuselage spars and wing ribs are formed (Figure 6(d)) before transverse structural components such as fuselage frames and wing spars are built (Figure 6(e)). After the construction of internal structural components is accomplished, upper and lower skins are generated sequentially, as shown in Figure 6(f) and (g).
- 4) Finally, the modeling of the internal structure and external skin of the entire tailless fighter wing is complete. Since only surfaces are needed for creating shell elements in FEA, the previously created key points and spline curves need to be hidden, as shown in Figure 6(f). Now that the entire structural modeling process is complete, the created surface model can be exported in IGES format for use in FEA. When conducting structural optimization design, all objects need to be erased after outputting the IGES model to generate new models for the next set of parameters.

Input: Template, plane and section parameters

Output: IGES model

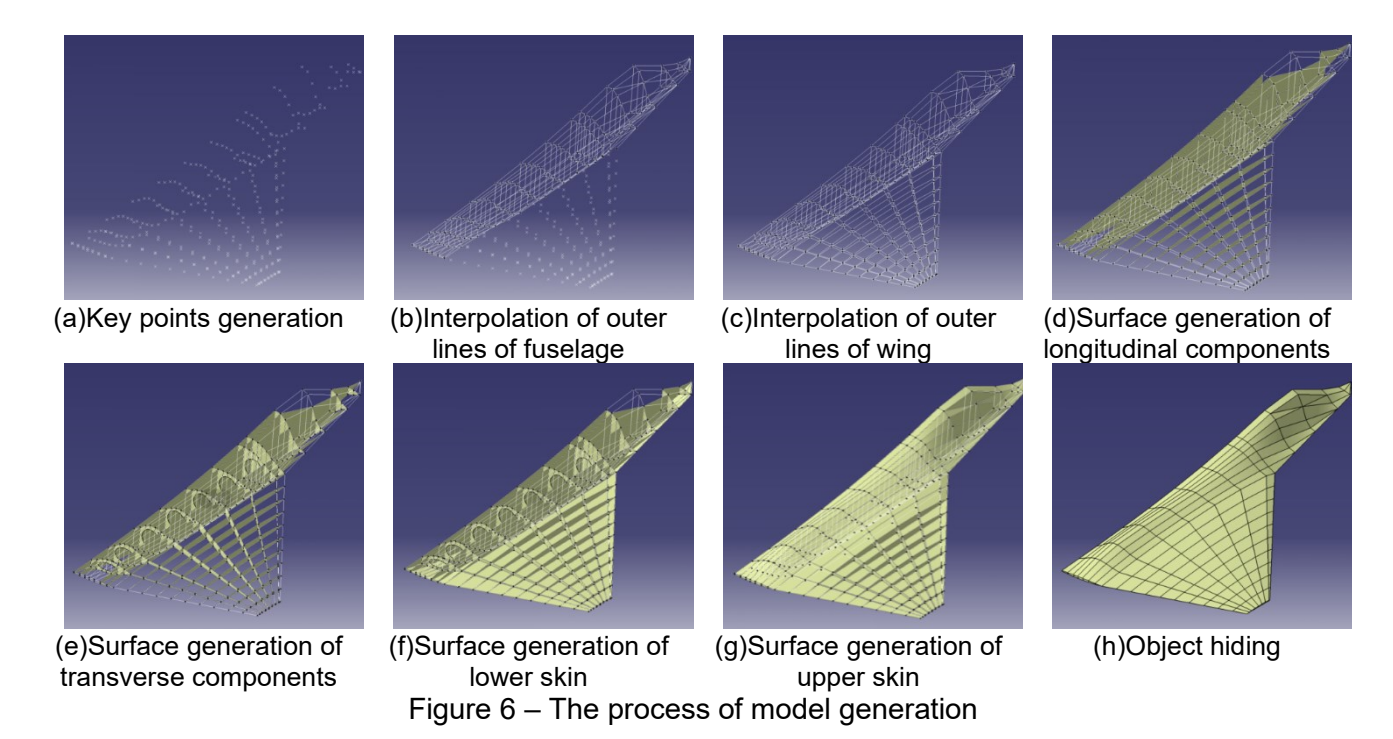
Begin

Generate key points

Connect the key points to form outer lines

Fill surfaces of inner structure
Fill surfaces of outer skin
Hide key points and outer lines

End



4. Validation

The proposed method facilitates more efficient modeling, however, it may compromise precision to a certain degree. This section aims to validate it by comparison with the manual fine-mesh model. The model generated by this method is a low-precision model, in which some intricate curves are approximated by multiple short straight lines. Additionally, a quadrilateral free mesh is employed during the FEA meshing stage, allowing for fewer triangular meshes and enabling rapid and automated grid generation. In contrast, the high-precision model employs manually partitioned mapped meshes, ensuring that all meshes are composed of regular quadrilaterals with aspect ratios close to 1, resulting in enhancing computational accuracy. Figure 7 illustrates the distinction between finite element meshes of two methods.

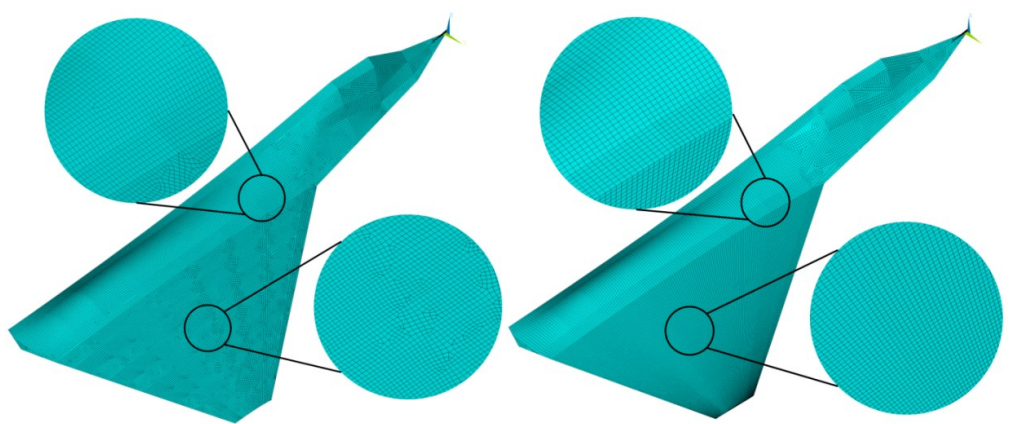
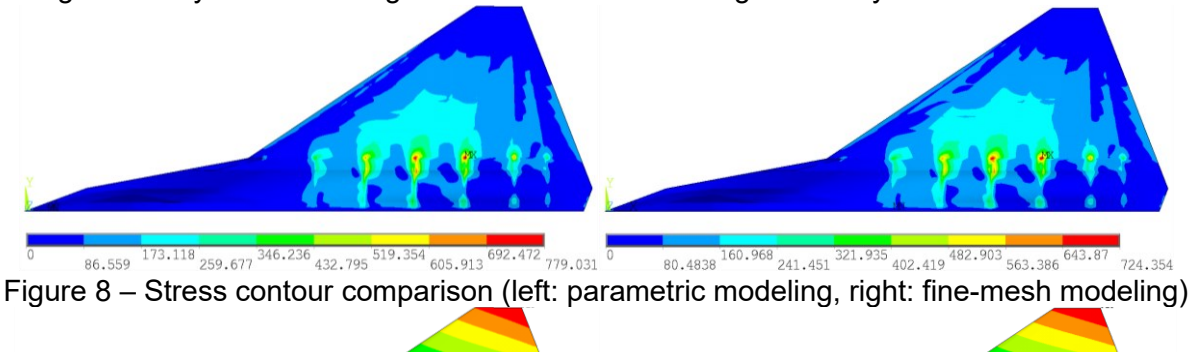


Figure 7 – FE mesh comparison (left: parametric modeling, right: fine-mesh modeling)

The stress and Y-deformation contours are shown in Figure 8 and 9. The FEA results are compared in Table 2. It is shown that this parametric method exhibits acceptable accuracy in stress, deformation, and weight calculations, which indicates satisfactory precision for conceptual design. Moreover, compared to traditional empirical formulas and statistical data, this parametric method offers higher fidelity while enabling fast and efficient modeling and analysis.



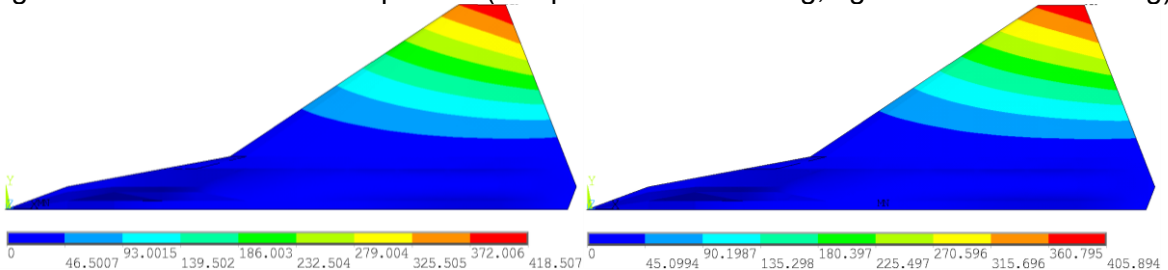


Figure 9 – Deformation contour comparison (left: parametric modeling, right: fine-mesh modeling)

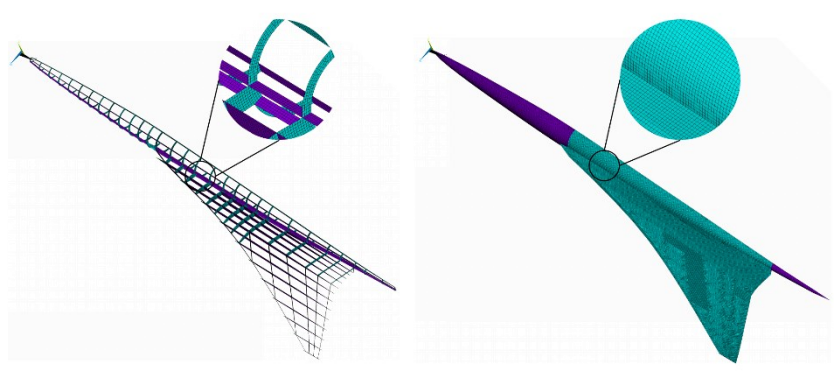
Table 2 – FEA results comparison

	Maximum stress	Maximum deformation	Structure weight
Parametric Modeling	779 MPa	418 mm	3636 kg
High-Precision Modeling	724 MPa	405 mm	3639 kg
Error	7.54%	3.11%	0.082%

5. Applications

5.1 FEA in variety of aircraft configurations

In this section, the fast parametric structural modeling method proposed in this paper is applied to the structural design of various configurations of aircraft, such as SST, tailless fighter, and flyingwing bomber. To verify the rationality of the structural design, FEA is performed on models of the three layouts. The primary steps include material assignment, section setting, meshing, load and boundary condition application, solving, and post-processing. Figures 7, 10, and 11 depict the internal and external meshes of the tailless fighter, supersonic airliner, and flying wing bomber. From the figures, it can be observed that the majority of meshes in the three models consist of regular quadrilateral grids with aspect ratios close to 1. This is because the surface discretization modeling preprocesses the geometric surfaces, dividing the entire complex and irregular surface into multiple regular quadrilaterals, thereby achieving automated meshing and improving mesh quality.



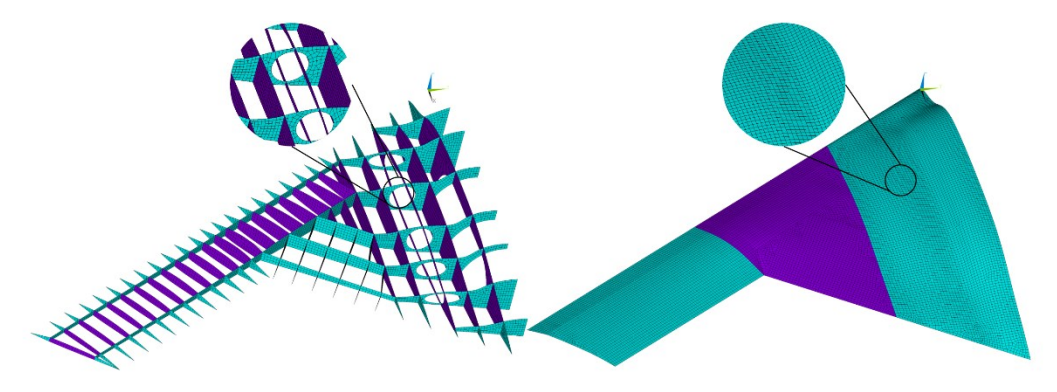


Figure 10 – The internal and external meshes of the supersonic airliner and flying wing bomber

The stress contour maps and deformation contour maps of the supersonic airliner, tailless fighter, and flying wing bomber are shown in Figures 11, respectively. From the figures, it can be observed that due to the large bending moment at the wing root, all three layouts exhibit high-stress regions at the wing roots, with noticeable stress concentrations at the weaker sections of the internal frames.

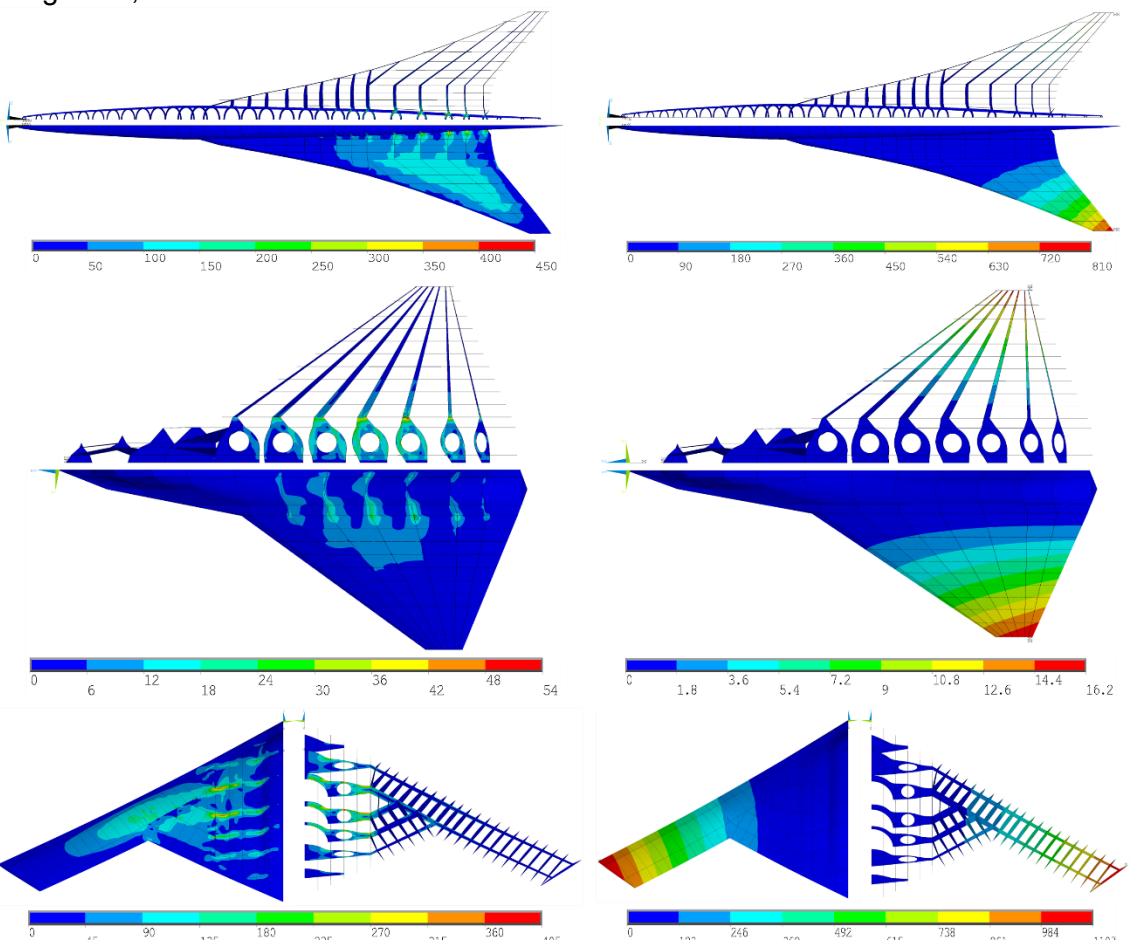


Figure 11 – Stress contour map (Left) and displacement contour map (Right) of the SST, tailless fighter and flying-wing bomber

5.2 Structural optimization

Based on the finite element structural analysis mentioned above, the parametric method proposed in this paper is employed to optimize the structures of three models. Thanks to the discretized surface modeling method, it is easy to divide the optimization design regions. By considering the different force states in each region, the optimal thickness is designed to maximize the utilization of materials through thickness optimization, ensuring that as much material as possible operates under relatively high stress to achieve the ultimate objective of reducing structural weight. The skin is divided into several design regions along the span, and the internal structure is divided into several design regions according to component types, with the thickness of each region as the design variable.

The design regions are divided according to the structural layout and stress characteristics of the SST in order to build a model for optimizing thickness. Figure 12 displays the design regions of the wing structure of the SST, with each hue representing a specific design zone. First, the wing's upper and lower skins are separated into six design zones along the span to account for the rising bending moment from tip to root, which increases internal structural stress. Next, spar design zones are divided. There are many spars due to the low aspect ratio and high taper ratio wing, and finite element analysis shows considerable stress changes at different positions. Based on the above stress characteristics, spars are separated into seven design zones. Since these six spars have varying lengths and heights, their stress states are very distinct, hence each is a unique design region. The remaining six spars are thin and kinked. Since these six spars have varying lengths and heights, their stress states are very distinct, hence each is a unique design region. All ribs are chosen as one design area since span and chord stress variation is negligible. Other structural components, such as fuselage longerons, bulkheads, and skins, are each designated as one design area. According to this design region division method, the wing has 23 design regions for thickness optimization: six on the upper surface, six on the lower surface, seven for the spars, one for the ribs, one for the fuselage skin, one for the bulkheads, and one for the longerons.

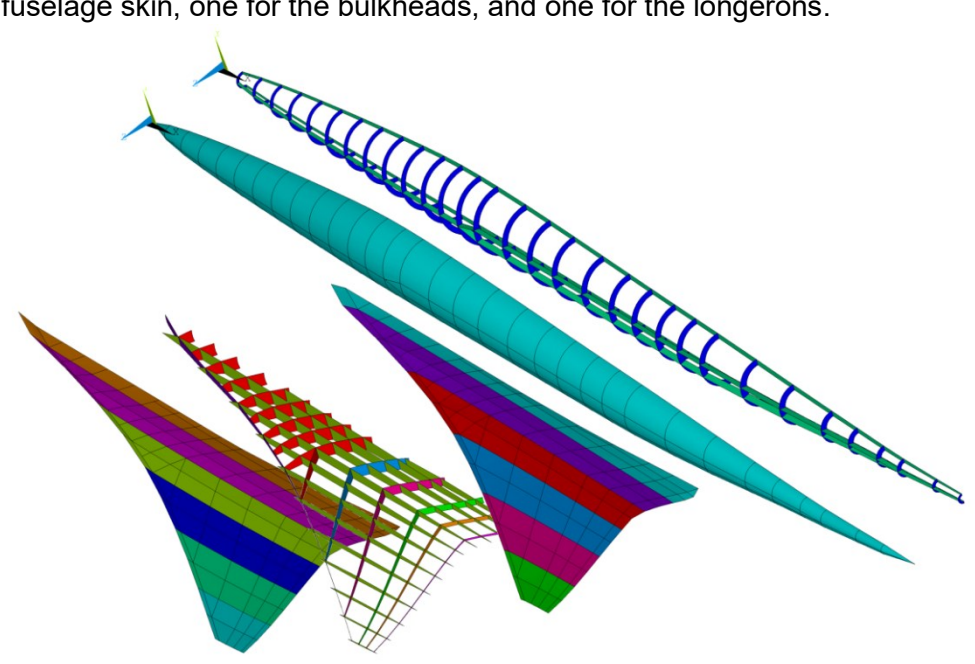


Figure 12 - Division of Design Areas for the Wing of SST

Based on the design regions mentioned above, thickness optimization design is conducted to find the optimal thickness distribution for each region, aiming to minimize the weight of the structure. The optimization mathematical model for this can be described as:

$$Min W = \rho \sum_{i=1}^{23} s_i t_i$$

$$s.t. KS(\sigma) \le 0$$

$$\delta_{tip} \le [\delta]$$

$$f_{Tsai-Wu} \le 1$$

$$\lambda \ge 1$$

$$t_{lb} \le t_i \le t_{ub} (i=1,2,\cdots 23)$$

$$(1)$$

In Equation (1), W represents the structural weight; ρ denotes the material density of the carbon fiber laminate; s_i signifies the area of the i-th design region; t_{lb} and t_{ub} respectively denotes the lower and upper limits constraints of the variables. In the wing structure, due to the different stress conditions in each region, the upper and lower limits of the thickness variables need to be set separately. $KS(\sigma)$ represents the allowable stress, obtained by accumulating the stresses of all nodes of the wing structure using the KS function, considering a safety factor of 1.5 and a carbon fiber laminate strength

of 1170 MPa, resulting in a final allowable stress of 780 MPa. $[\delta]$ denotes the maximum displacement constraint of the wing, with a maximum deformation of 700 mm for the supersonic wing model. $f_{Tsai-Wu}$ represents the Tsai-Wu failure criterion for composite wings, which should not exceed 1; otherwise, it indicates failure of the composite material. λ denotes the buckling eigenvalue of the upper and lower wing surfaces, which should not be less than 1, indicating that the wing skin will not experience buckling instability under the current load.

Based on the thickness optimization model for SST, the Latin hypercube method is employed to generate sample points within the design space, with an initial setting of 60 sample points. The El criterion is used for updating the surrogate model, with a maximum of 200 sample points set as the condition for iterative convergence. The optimization iteration convergence curve is shown in Figure 13.

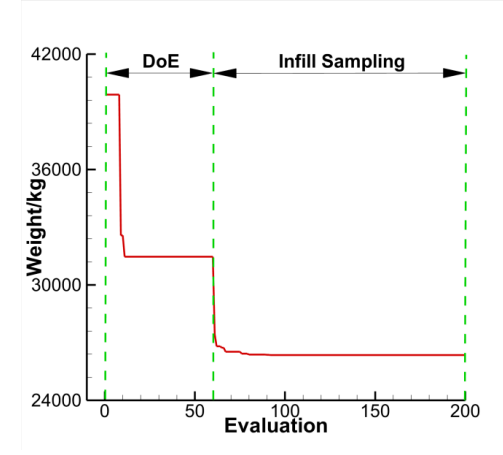


Figure 13 – Convergence curve of thickness optimization iterations for the wing layup of SST

Following thickness optimization, the thickness of each section was reallocated, significantly lowering the structural weight. The structure's convergent weight after optimization is 26,407.03 kg, which is 26.5% lighter than its initial weight of 35,934.43 kg, demonstrating a considerable weight reduction result. Figure 14 depicts the thickness distribution of SST structures in each location. The figure shows that the upper and lower wing skins have significantly different thicknesses, with the top wing skin being thicker than the lower wing skin. This phenomenon is caused by the top and lower wing skins being subjected to differing forces. The lower wing skin is in tension due to lift force, but the upper wing skin is in compression. Compression loads can cause buckling instability in thinwalled structures such as skins. As a result, in the optimization phase, thicker upper wing skins are considered to meet buckling limitations.

Furthermore, the thickness of the upper and lower wing skins does not drop linearly from the wing root to the wingtip, but rather increases and subsequently decreases. This differs from the basic design, in which the skin thickness falls linearly across the span. The analysis finds that this is related to the SST wing's unique layout features. The wing has a small aspect ratio and a large taper ratio, with the root chord significantly greater than the tip chord. As a result, the wing root skin has a larger loaded cross-sectional area to resist the skin tension and compression loads induced by bending. The increased loaded cross-sectional area will help minimize stress on the skin. The bending moment gradually increases from the wing tip to the wing root, but the large taper ratio increases the loaded cross-sectional area more, reducing inner skin stress. Furthermore, the wing root has a thicker airfoil and a higher spar height, increasing the wing structure's bending resistance and capabilities. As a result, the thickness of the top and lower skins increases initially and then lowers along the span.

There are significant changes in the thickness of internal structural components. From the Figure 14, it can be seen that the thickness of the leading edge triangular region beams is small, while the thickness of the 5 longer trailing edge beams significantly increases. This is because the triangular region experiences less force, with lift mainly concentrated in the trailing edge section of the wing, and the height of the 5 longer trailing edge spars is small, leading to a decrease in the bending stiffness coefficient, which can only be compensated by increasing the thickness to reduce structural stress. A similar situation occurs above the fuselage bulkheads, where the wings directly transmit

loads to the fuselage bulkheads, and due to the limited cabin space, the height of the frames in the mid-fuselage is small, resulting in relatively large forces on the mid-fuselage bulkheads. Therefore, it is necessary to increase the thickness of the bulkheads to avoid stress concentration. The fuselage longerons and fuselage skin, due to the relatively small longitudinal loads they experience, have a thinner thickness.

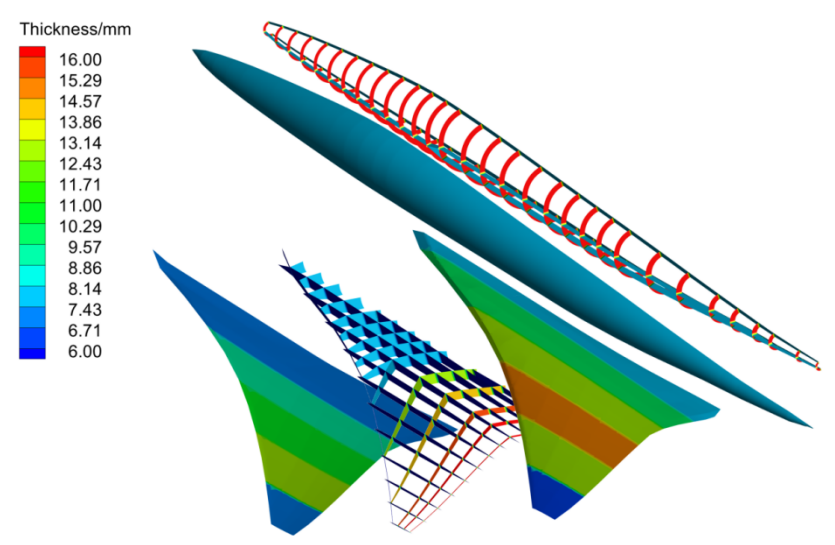


Figure 14 – The thickness distribution of various design regions of SST

The stress and displacement comparisons of the wing skin before and after optimization are shown in Figure 15. From the stress contour plot, it can be observed that the high-stress areas at the wing root increase after optimization, but still meet the maximum stress constraint. This is consistent with the trend of thickness variation shown in Figure 14, indicating a thinning of the skin at the wing root. From the displacement contour plot, it is evident that the overall deformation of the wing increases after optimization but still remains within the range of the maximum deformation constraint. This phenomenon occurs as a result of the reduction in the overall rigidity of the wing due to the thinning of the skin in specific areas. Consequently, the wing gradually deforms until it reaches the maximum deformation limit at its boundary. From the comparison of stress and displacement of the supersonic civil aircraft wing, as well as the thickness distribution, it can be concluded that the optimization of ply thickness redistributes the thickness of each partition of the wing structure, adjusting the thickness according to the stress characteristics of each region. This maximizes the utilization of materials and ultimately achieves the objective of reducing weight.

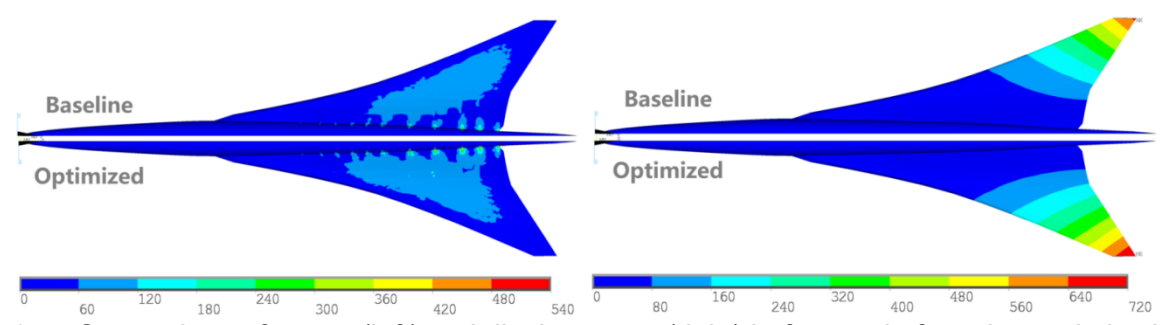


Figure 15 – Comparison of stress (left) and displacement (right) before and after wing optimization

The parameters before and after optimization of the wing of the SST are shown in Table 1. The table clearly demonstrates that the wing's structural weight fell by 26.5% after two levels of optimization. The stress and deformation saw a simultaneous rise, however, they stayed within the specified limits. The Tsai-Wu failure index approached 1, indicating that the material was subjected to higher stress levels within the strength constraints, thus improving material utilization efficiency. The buckling eigenvalue of the wing also became closer to 1, indicating that during the optimization process, it was subjected to constraints on buckling, ensuring structural stability during weight reduction.

Table 3 – The comparison of various parameters before and after optimization of the SST

	Weight/Kg	σ_{max} /MPa	δ_{max} /mm	$f_{Tsai-Wu}$	$\lambda_{buckling}$
Baseline	35934.43	468.17	660.29	0.69	2.12
Optimized	26407.03	569.51	727.24	0.99	1.01
Variation	↓ 26.5%	↑21.6%	↑10.1%	-	-

6. Conclusion and Outlook

This work presents a fast parametric method for simulating a wide range of entire aircraft configurations. Firstly, a novel method of surface discretization modeling is proposed. Research indicates that surface discretization modeling greatly facilitates subsequent FE meshing and design area division. Furthermore, this structural parametric method is elaborated upon in terms of its conceptual framework, program modules, input design parameters, and modeling procedures. An automated modeling process for structures is achieved. Subsequently, the accuracy of this method is verified by comparison with high-precision models. Results demonstrate that this parametric method provides acceptable accuracy in stress, deformation, and weight calculations, satisfying the criteria of aircraft conceptual and preliminary design. Finally, the SST, tailless fighter, and flying wing bomber are designed using this paper's structural parametric method. Finite element analysis evaluates structural design rationality in models developed using this method. Skin and internal components are split into design zones, with thickness as a design variable for structural dimension optimization of the three configurations. The surface discretization modeling method allows for the easy partitioning of optimization design areas, enabling rapid and flexible structural optimization designs for various aircraft configurations.

This work suggests that the proposed parametric structure modeling is an efficient approach for the structural design of aircraft during the conceptual design stage. A lot of simplification is made to the wings during parameterization modeling, such as using the smearing stiffness method to equivalence the wing truss. The wing truss stiffness is represented by an increase in skin thickness. While this approach does streamline the process of modeling the truss, it may compromise the accuracy of finite element analysis. In future research, it is recommended to explore more refined wing structural models and corresponding parametric modeling methods to address the requirements of conducting local buckling analysis.

7. Acknowledgment

This research was sponsored by the Aeronautical Science Fund under Grant No.20230014053006, the National Key Research and Development Program of China under Grant No. 2023YFB3002800, the National Natural Science Foundation under Grant No.U20B2007. The authors are members of The Youth Innovation Team of Shaanxi Universities.

8. Contact Author Email Address

Yunlong Yin: 2021260229@mail.nwpu.edu.cn Keshi Zhang: zhangkeshi@nwpu.edu.cn Hailong Qiao: qiaohailong@mail.nwpu.edu.cn Ailing Che: che_ailing@mail.nwpu.edu.cn Zhonghua Han: hanzh@nwpu.edu.cn

9. Copyright Statement

The authors confirm that they, and/or their company or organization, hold copyright on all of the original material included in this paper. The authors also confirm that they have obtained permission, from the copyright holder of any third party material included in this paper, to publish it as part of their paper. The authors confirm that they give permission, or have obtained permission from the copyright holder of this paper, for the publication and distribution of this paper as part of the ICAS proceedings or as individual off-prints from the proceedings.

References

- [1] Siggel M, Kleinert J, Stollenwerk T, et al. TiGL: an open source computational geometry library for parametric aircraft design. *Mathematics in Computer Science*, Vol. 13, No.3, pp 367-389, 2019.
- [2] Alder M, Moerland E, Jepsen J, et al. Recent advances in establishing a common language for aircraft design with CPACS. *Aerospace Europe Conference 2020*, Bordeaux, Frankreich, 2020.
- [3] Freund S, Heinecke F and Führer T. Parametric model generation and sizing of lightweight structures for a multidisciplinary design process. *NAFEMS DACH-Tagung*, pp 20-21, 2014.
- [4] Klimmek T. Parameterization of topology and geometry for the multidisciplinary optimization of wing structures. *CEAS 2009 European Air and Space Conference*, Manchester, United Kingdom, 2009.
- [5] Führer T, Willberg C and Freund S, et al. Automated model generation and sizing of aircraft structures. Aircraft Engineering and Aerospace Technology: An International Journal, Vol. 88, No. 2, pp 268-276, 2016
- [6] Wunderlich T and Dähne S. Aeroelastic tailoring of an NLF forward swept wing: DLR contribution to LuFo IV joint research project AeroStruct. *CEAS Aeronautical Journal*, Vol 8, No. 3, pp 461-479, 2017.
- [7] Voß A and Klimmek T. Parametric aeroelastic modeling, maneuver loads analysis using CFD methods and structural design of a fighter aircraft. *Aerospace Science and Technology*, Vol 136, 2023.
- [8] Klimmek T, et al. cpacs-MONA–An independent and in high fidelity based MDO tasks integrated process for the structural and aeroelastic design for aircraft configurations. *International Forum on Aeroelasticity and Structural Dynamics* 2019, 2019.
- [9] McDonald R A and James R G. Open vehicle sketch pad: An open source parametric geometry and analysis tool for conceptual aircraft design. *AIAA SciTech 2022 Forum*, 2022.
- [10]Weitsman D and Eric G. Parametric study of eVTOL rotor acoustic design trades. *AIAA Scitech 2021 Forum*, 2021.
- [11]Winter T F, Joe R, Armando G and Thomas N. Conceptual Design Structural Sizing for Urban Air Mobility. *AIAA Scitech 2021 Forum*, pp 1722, 2021.
- [12] Ayele W, McEntire C, et al. Conceptual Design of a Robotic Ground-Aerial Vehicle for Mars Planetary Exploration. *AIAA AVIATION 2022 Forum*, pp 3285, 2022.
- [13]Kumar S M, Okasha M, et al. Dynamic Stability of a Blended Wing Body Unmanned Aerial Vehicle. 2023 Advances in Science and Engineering Technology International Conferences (ASET). pp 1-9, 2023.
- [14]Hwang J, Kenway G and Martins J R R A. Geometry and structural modeling for high-fidelity aircraft conceptual design optimization. *15th AIAA/ISSMO Multidisciplinary Analysis and Optimization Conference*, 2014.
- [15]Kenway G K W, Kennedy G J and Martins J R R A. Scalable parallel approach for high-fidelity steady-state aeroelastic analysis and adjoint derivative computations. *AIAA journal*, Vol. 52, No. 5, pp 935-951, 2014.
- [16] Joe J, Gandhi V, Dannenhoffer J, et al. Rapid generation of parametric aircraft structural models. *AIAA SciTech 2019 Forum*, San Diego, California, 2019.
- [17] Haimes R. and Dannenhoffer J. The Engineering Sketch Pad: A Solid-Modeling, Feature-Based, Web-Enabled System for Building Parametric Geometry. 21st AIAA Computational Fluid Dynamics Conference, American Institute of Aeronautics and Astronautics, 2013.
- [18]Corrado G, Ntourmas G and Sferza M. Recent progress, challenges and outlook for multidisciplinary structural optimization of aircraft and aerial vehicles. *Progress in Aerospace Sciences*, Vol. 135, pp 100861, 2022.
- [19]Laan A H and Van Tooren M J L. Parametric modeling of movables for structural analysis. *Journal of aircraft*, Vol. 42, No. 6, pp 1605-1613, 2005.
- [20]Zhu W S, Fan Z W and Yu X Q. Structural mass prediction in conceptual design of blended-wing-body aircraft. *Chinese Journal of Aeronautics*, Vol. 32, No. 11, pp 2455-2465, 2019.
- [21]Yin H L and Yu X Q. Integration of manufacturing cost into structural optimization of composite wings. *Chinese Journal of Aeronautics*, Vol. 23, No. 6, pp 670-676, 2010.
- [22]Hu T Y and Yu X Q. Aerodynamic/Stealthy/Structural Multidisciplinary Design Optimization of Unmanned Combat Air Vehicle. *Chinese Journal of Aeronautics*, Vol 22, No. 4, pp 380-386, 2009.